Supporting Information

Configuration-Regulated Highly Luminescent Hydrogen–Organic Frameworks for Detection of Phenelzine and Propofol

Yanhong Liu,† Bing Yan*†

†School of Chemical Science and Engineering, Tongji University, 1239 Siping Road, Shanghai 200092, China

* Corresponding author: Bing Yan, Email: byan@tongji.edu.cn

Experimental Section

Materials and instruments:

Tris(4-(pyridin-4-yl)phenyl)amine (TPPA, 98%) was from Yanshen Technology Co., Ltd, China. All other reagents and solvents were commercially available and used as received without further purification. The crystalline phases of the samples were determined by Powder X-ray diffraction patterns (PXRD) on a Bruker D8 diffractometer with Cu Kα radiation (40 kV, 40 mA) over the range of 5 ~ 50° at a scan rate of $0.1°\cdot S^{-1}$. Simulation of the PXRD spectra was carried out by the single-crystal data and diffraction-crystal module of the Mercury program. Thermogravimetric analyses (TGA) were conducted on a PerkinElmer thermogravimetric analyzer from 30 to 800 °C at a rate of 10 $°C\cdot min^{-1}$ in flowing N_2. Fourier transform infrared (FT-IR) spectra were recorded using a Nicolet IS10 infrared spectrophotometer. The fluorescence spectra were examined on an Edinburgh FLS920 fluorescence spectrometer at room temperature. ^1H nuclear magnetic resonance (^1H NMR) spectra of the dissolved sample (diluted d-DMSO) were recorded on a Bruker Avance III 400. The corresponding Commission Internationale de I'Eclairage (CIE) color coordinates were calculated based on the international CIE standards.

Single-crystal X-ray Crystallography

The crystal structure of the as-prepared single crystal was analyzed using a Bruker SMART APEX II CCD area detector X-ray diffractometer, applying Mo Kα radiation (λ = 0. 71073 Å) at 50 kV and 30 mA. The structures were solved by direct methods and refined by full-matrix least-squares methods on all F^2 data (Olex2). Non-hydrogen atoms were refined anisotropically. The positions of hydrogen atoms were calculated and refined isotropically. Crystal parameters and details of refinements are given in Table S1 and S2.

Computational methods of DFT

Density functional theory (DFT) calculations were carried out by using the Gaussian 09 package [1]. The ground-state geometries were extracted from their crystalline structures. The excited-state geometries of these molecules were directly optimized using the time-dependent density functional theory (TDDFT) with CAM-B3LYP functional and 6-31G(d,p) basis set. The implicit solvation models (SMD) of water and the dispersion corrections with Grimme's D3 method [2] were taken into consideration in all calculations.

Preparation of TPPA-BDC: Tris(4-(pyridin-4-yl)phenyl)amine (TPPA, 0.012 g, 0.025 mmol) and 1,4-Benzenedicarboxylic acid (H_2BDC, 0.013 g, 0.075 mmoL) were mixed into a 5 mL methanol solution to form a mixture, which was treated with ultrasound for 2 min. The mixture was added to a Teflon-lined steel autoclave and kept in an oven at 80 °C for 24 h. After that, the reaction system was cooled to room temperature. The bright yellow crystals of TPPA-BDC collected by filtration were washed several times with the original solution and dried in air.

Preparation of TPPA-BTC: Tris(4-(pyridin-4-yl)phenyl)amine (TPPA, 0.048 g, 0.1

mmol) and 1,3,5-benzenetricarboxylic acid (H_3BTC, 0.053 g, 0.25 mmoL) were mixed into a 20 mL methanol solution to form a mixture, which was treated with ultrasound for 5 min. The mixture was heated for about 3 h at 60 °C, yellow block crystals can be acquired.

Preparation of TPPA-H_2O: The suspension of TPPA-BDC soaked in phenlzine (PZ) was centrifuged and washed with deionized water, and the solid powder obtained was dried. The dried solid powder was dissolved in ethanol (1 mL) and sonicated for 5 min, then deionized water (1 mL) was added and evaporated at room temperature for 5 days to obtain light yellow needle-like crystals.

Procedures for phenelzine (PZ) and propofol (PPF) detection: In a typical assay for PEA using the sensory material, 0.5 mg of TPPA-BDC ground powders were weighed and added to a 1.5 mL centrifuge tube containing the deionized water (1 mL) and a series of concentrations of fresh PZ aqueous solution (10^{-5}–10^{-3} M) or PPF aqueous solution (10^{-5}–10^{-2} M), followed by ultrasonication to form the uniform dispersion. Then, the prepared suspensions were transferred to fluorescence cuvettes with covers, and their luminescence spectra were measured in the 410–650 nm range under excitation at 360 nm. Test samples for the selectivity experiment were prepared with a similar procedure. Samples for specificity experiments were similarly prepared by adding TPPA-BDC into different chemicals mainly including (KCl, NaCl, lysozyme(Lys), NH_4Cl, $CaCl_2$, mucin, $MgCl_2$, α-amylase(Amy), Na_2CO_3, NaH_2PO_4, creatine(Cre), glucose(Glu), L-Proline(L-pro), $NaHCO_3$ and Na_2SO_4 10^{-2} M) in saliva and serum. These mixtures were then sonicated for luminescence measurements.

Saliva and urine sample preparation: The artificial saliva and serum samples were prepared using the reported procedures. [3]

Table S1. Crystal data and refinement parameters for **TPPA-BDC** and **TPPA-BTC**.

Identification code	**TPPA-BDC**	**TPPA-BTC**
Chemical formula	$C_{41}H_{30}N_4O_4$	$C_{42}H_{30}N_4O_6$
Formula weight	642.69	686.70
Crystal Colour	Yellow	Yellow
Temperature (K)	100	150
Crystal System	Monoclinic	Triclinic
Space Group	$C2/c$	*P*-1
a(Å)	22.5474(12)	11.6130(6)
b(Å)	12.5664(8)	13.3303(7)
c(Å)	22.7995(14)	15.7331(7)
α(°)	90	93.278
β(°)	100.306	102.022
γ(°)	90	106.557
Z	8	2
V(Å^3)	6355.8(7)	2265.7(2)
D_{calc}(g cm^{-3})	1.343	1.007
F(000)	2688	716
R(int)	0.0850	0.0855
Number of parameters	443	767
GOF on F^2	1.047	1.049
$R1^a$[I>2δ(I)]	0.0872	0.0820
wR_2^b(all data)	0.0999	0.1829
CCDC	2205391	2205392

$R_1 = \Sigma(||Fo| - |Fc||)/\Sigma|Fo|$; $wR_2 = \{\Sigma w(|Fo|^2 - |Fc|^2)^2/\Sigma w(|Fo|^2)^2\}^{1/2}$.

Table S2 Crystal data and refinement parameters for **TPPA-H_2O**.

Identification code	**TPPA-H_2O**
Chemical formula	$C_{33}H_{28}N_4O_2$
Formula weight	512.59
Crystal Colour	Yellow
Temperature (K)	121
Crystal System	Monoclinic
Space Group	*P*21/c
a(Å)	10.0367(4)
b(Å)	23.407(1)
c(Å)	12.1733(5)
α(°)	90.000
β(°)	113.958
γ(°)	90.000
Z	4
V(Å^3)	2613.5(2)
D_{calc}(g cm^{-3})	1.307
F(000)	716
R(int)	0.062
Number of parameters	358
GOF on F^2	1.048
$R1^a$[I>2δ(I)]	0.0408
wR_2^b(all data)	0.097
CCDC	2256002

$R_1 = \Sigma(||Fo| - |Fc||)/\Sigma|Fo|$; $wR_2 = \{\Sigma w(|Fo|^2 - |Fc|^2)^2/\Sigma w(|Fo|^2)^2\}^{1/2}$.

Table S3. Hydrogen bonds for TPPA-BDC

D–H···A [Å]	**d(D–H) [Å]**	**d(H···A) [Å]**	**d(D···A) [Å]**	**<(DHA) [°]**
O(3)-H(3A)···N(1)	0.84	1.76	2.584(2)	167.9
O(4)-H(4A)···N(4)$^{\#1}$	0.84	1.76	2.588(2)	168.7

Symmetry transformations used to generate equivalent atoms:
#1: 1-X, -2+Y, 1.5-Z;

Table S4. Hydrogen bonds for TPPA-BTC

D-H···A [Å]	**d(D-H) [Å]**	**d(H···A) [Å]**	**d(D···A) [Å]**	**<(DHA) [°]**
O(1)-H(1A)···N(3)$^{\#1}$	0.84	1.77	2.599(2)	170.6
O(5)-H(5A)···N(1)$^{\#2}$	0.84	1.72	2.555(2)	169.6
O(4)-H(4A)···N(4)$^{\#3}$	0.84	1.75	2.576(2)	166.4

Symmetry transformations used to generate equivalent atoms:
#1 x,y-1,z #2 x-1,y,z-1 #3 x+1,y+1,z

Table S5. Quantum yields (QY), fluorescence lifetimes (τ) and non-radiative rates (k) of TPPA-BDC and TPPA-BTC. $k = (1 - QY)/\tau$.

Sample	QY (%)	τ_1 (ns)	τ_2 (ns)	τ (ns)	k (S^{-1})
TPPA-BDC	25.45	1.89	15.01	11.82	6.31×10^7
TPPA-BTC	14.51	157	12.19	9.87	8.66×10^7

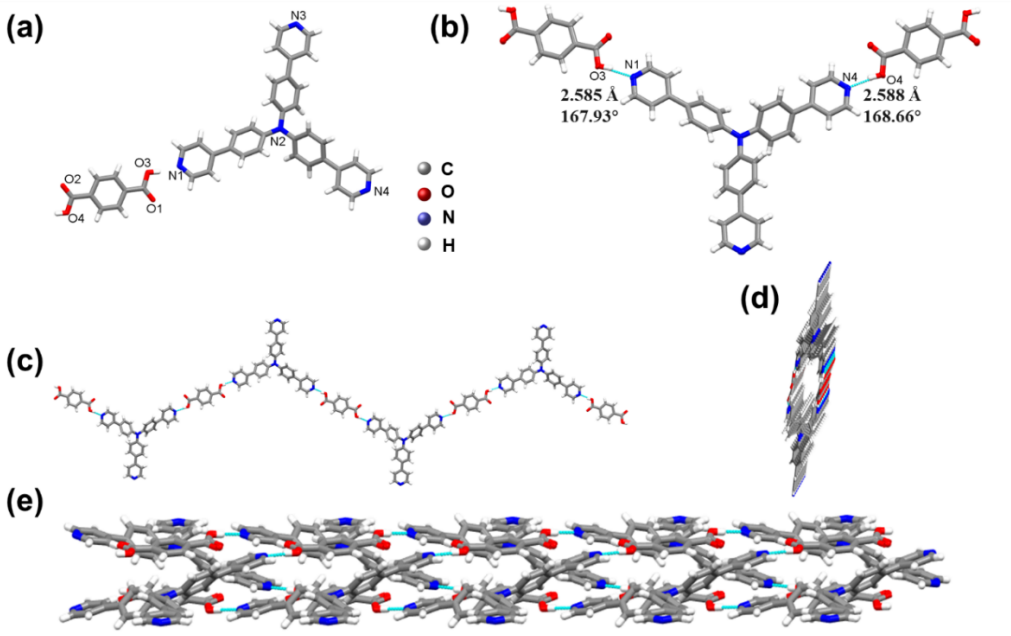

Fig. S1. The structural details of TPPA-BDC. (a) The asymmetric unit of TPPA-BDC, C = grey, O = red, N = blue and H = white. (b) The existence of two H_2BDC molecules around a TPPA molecule, forming O–H···N (cyan) hydrogen bonds. (c) Adjacent TPPA and H_2BDC molecules linked by O3–H···N1 and O4–H···N4 bonds form a one-dimensional (1-D) chain. (d) A 1-D channel along the b axis. (e) Adjacent four entangled 1-D chains connected by C–H···O weak hydrogen bonds.

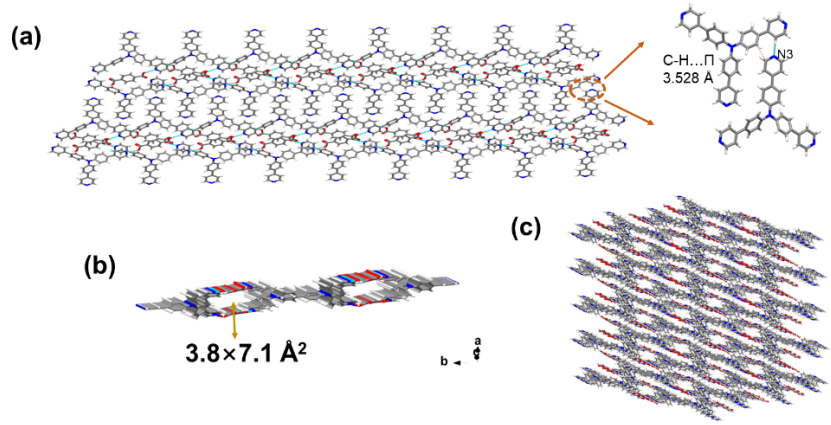

Fig. S2. (a) Adjacent structural units connect with each other to form a 2-D layer based on the C–H···N3 bonds and C–H···Π interaction along the bc plane. (b) The view of the 2-D layer along the b direction. (c) The three-dimensional (3-D) supramolecular structure formed by 2-D layers.

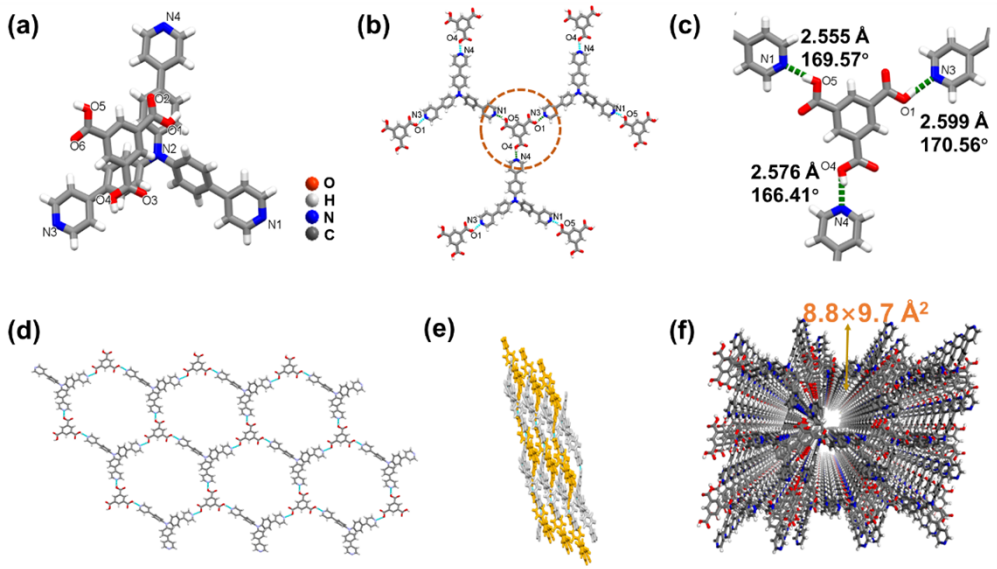

Fig. S3. The structural details of TPPA-BTC. (a) The asymmetric unit of TPPA-BTC, C = grey, O = red, N = blue and H = white. (b) The existence of three TPPA molecules around a H_3BTC molecule, forming O–H···N (cyan) hydrogen bonds (c). (d) Adjacent 1-D chain connect with each other to form a 2-D layer based on hydrogen bond interaction b axis. (e) The layers align in …ABAB…sequence along the b-axis. (f) The 1D channel in TPPA-BTC along the a-axis.

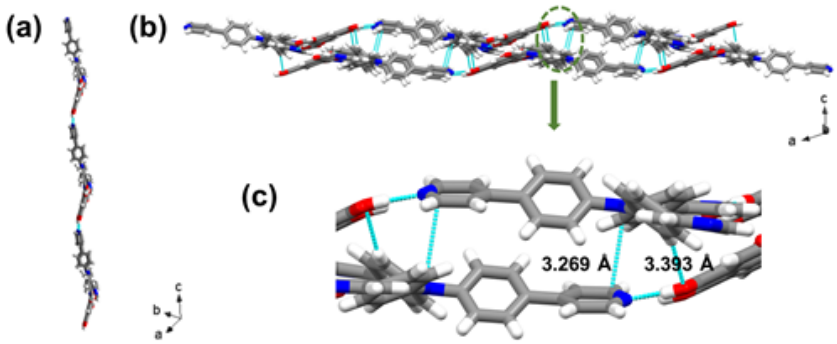

Fig. S4. (a) The polyline-type structure of a two-dimensional layer viewed along the ac plane. (b-c) The interaction between two adjacent two-dimensional layers.

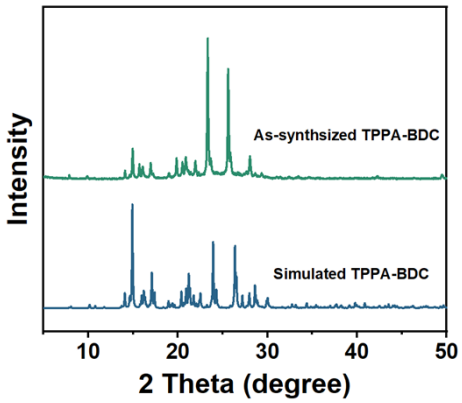

Fig. S5. PXRD patterns of simulated TPPA-BDC (blue) and synthesised TPPA-BDC (green).

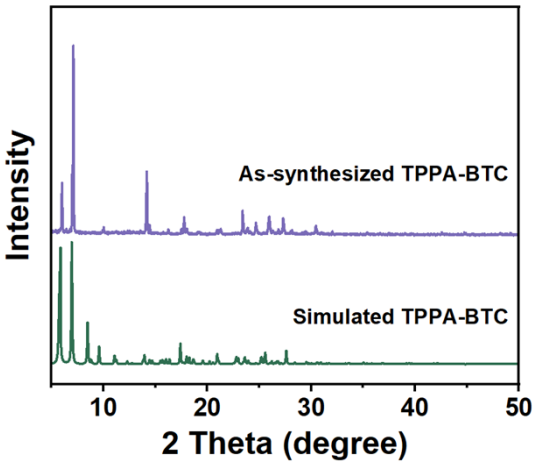

Fig. S6. PXRD patterns of simulated TPPA-BTC (green) and synthesised TPPA-BTC (purple).

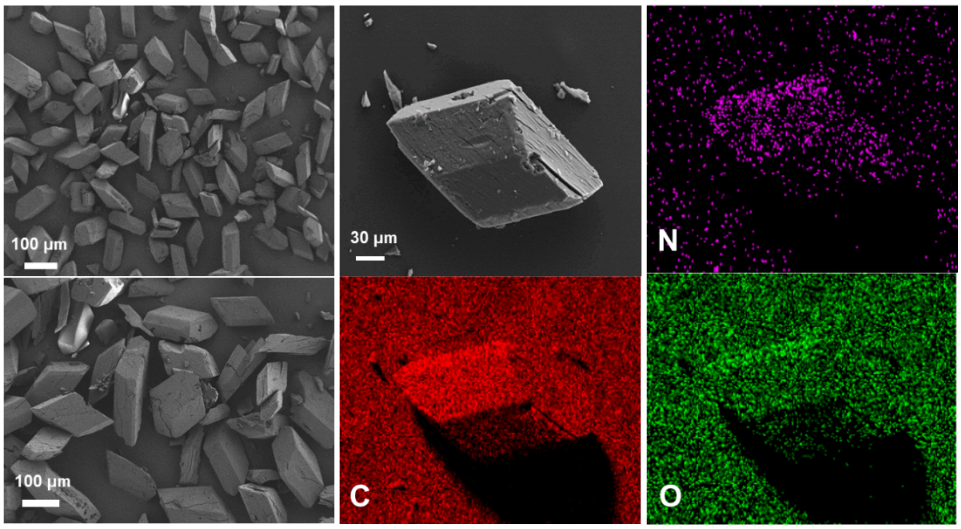

Fig. S7. SEM and elemental mapping images of TPPA-BTC.

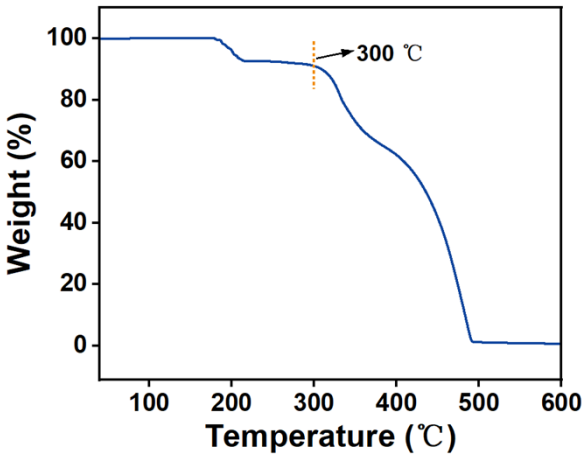

Fig. S8. TGA traces of TPPA-BDC ranging from room temperature to 600 ℃.

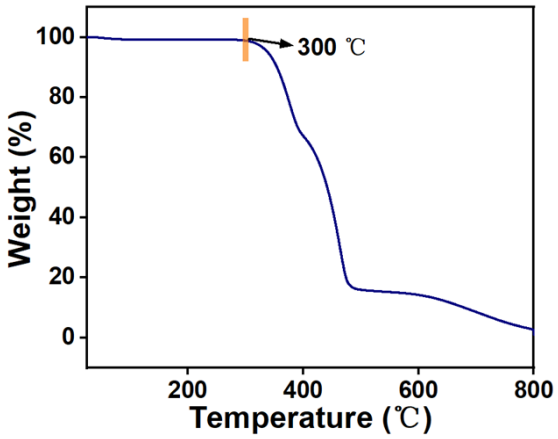

Fig. S9. TGA traces of TPPA-BTC ranging from room temperature to 800 ℃.

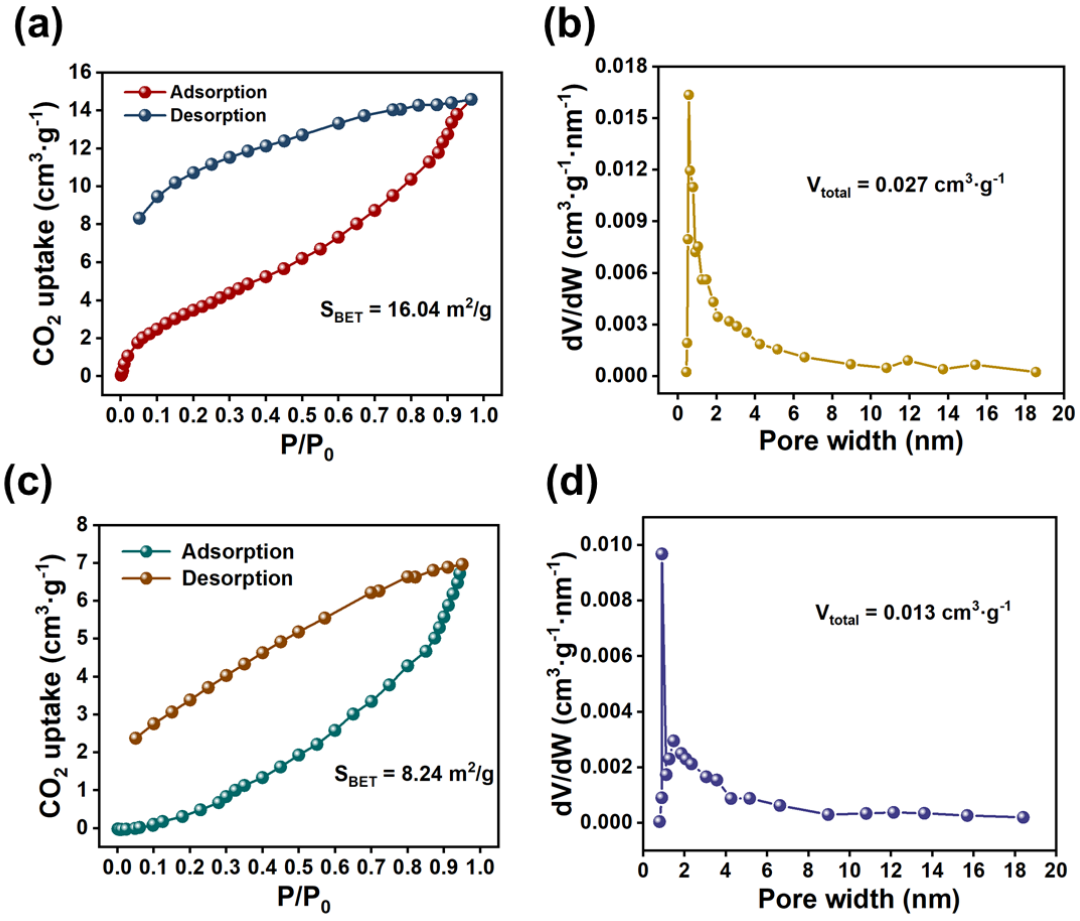

Fig. S10 (a) and (c) N_2 adsorption-desorption isotherm of TPPA-BTC and TPPA-BDC; (b) and (d) Pore size distribution of TPPA-BTC and TPPA-BDC.

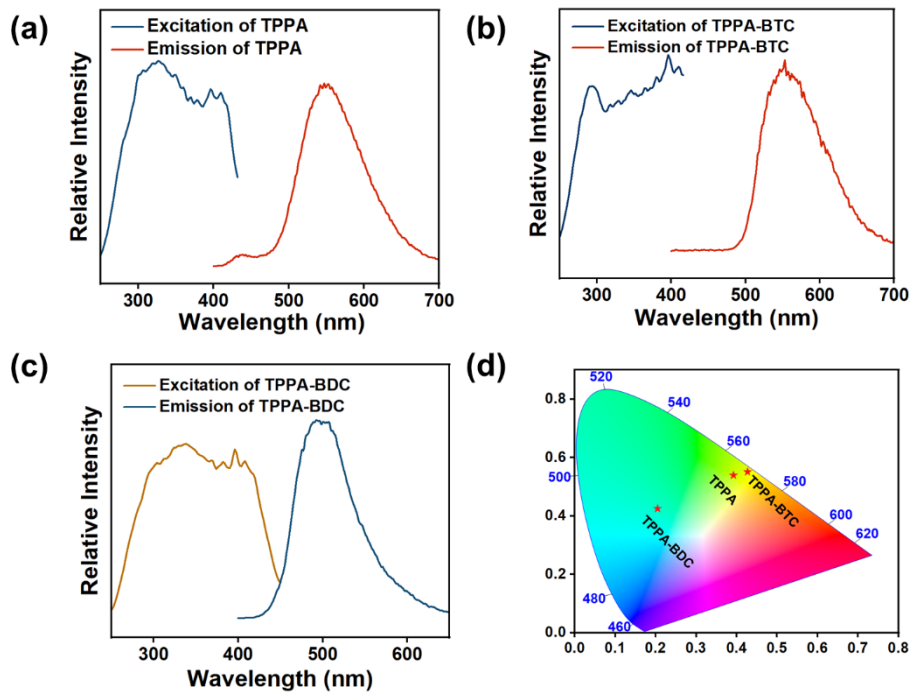

Fig. S11. The excitation and emission spectra of TPPA (a), TPPA-BTC (b) and TPPA-BDC (c) in aqueous solution. (d) The CIE chromaticity coordinates of TPPA, TPPA-BTC and TPPA-BDC in aqueous solution.

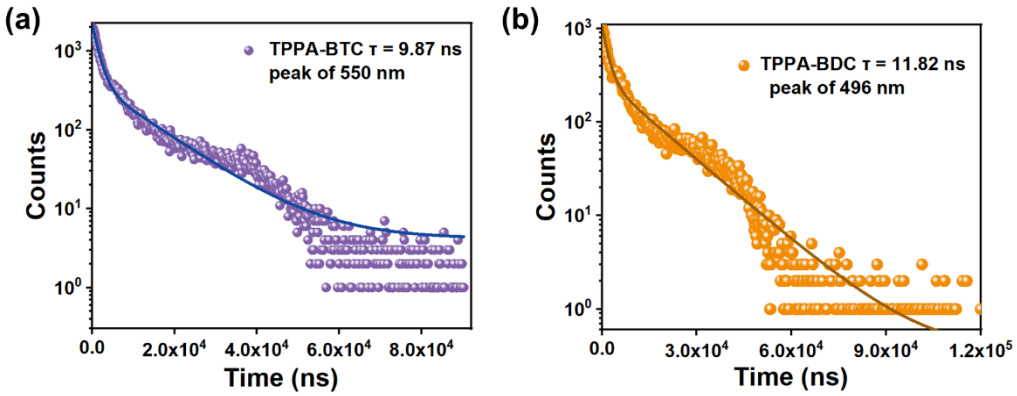

Fig. S12. Decay lifetimes of TPPA-BTC (a) and TPPA-BDC (b) (λex = 360 nm).

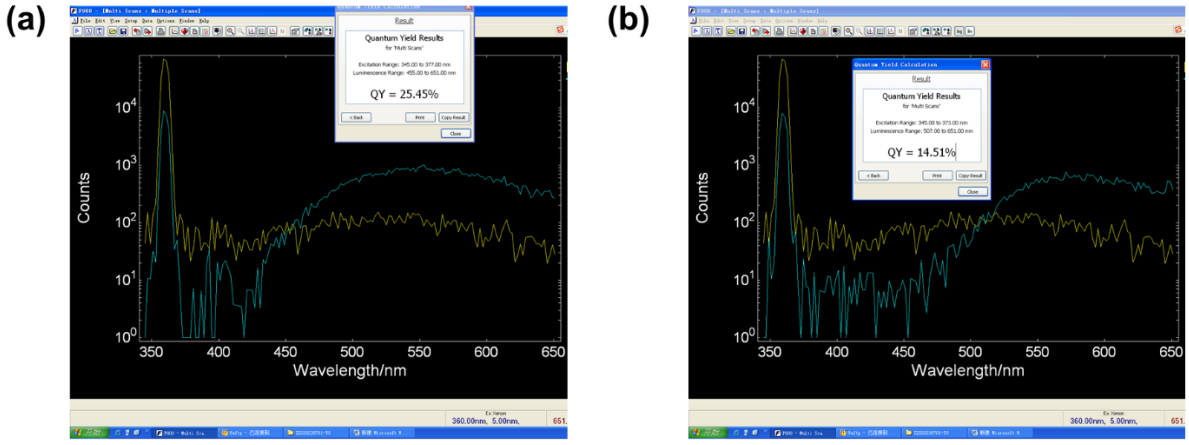

Fig. S13. Quantum yield of TPPA-BDC (a) and TPPA-BTC (b) (λex = 360 nm). The fluorescence quantum efficiency calculation formula is $Y_U = Y_S \cdot (F_U/F_S) \cdot (A_S/A_U)$. Y_U, F_U and A_U represent fluorescence quantum yield, integral fluorescence intensity and absorbance of the substance to be measured, respectively. Y_S, F_S and A_S represent fluorescence quantum yield, integral fluorescence intensity and absorbance of the reference substance, respectively.

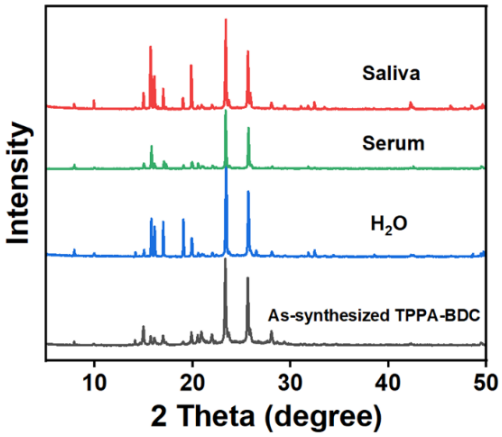

Fig. S14. PXRD patterns of TPPA-BDC after immersion in H_2O (blue), serum (green) and saliva (red).

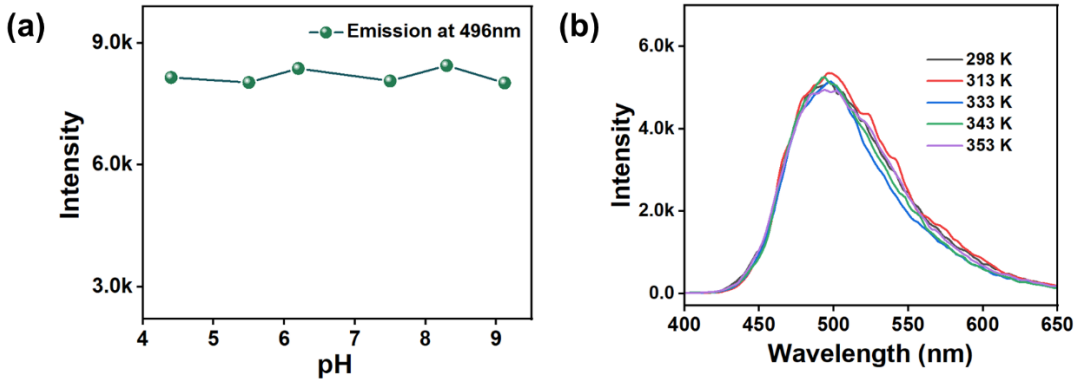

Fig. S15. (a) Effects of *p*H on the luminescence intensities of TPPA-BDC at 496 nm. (b) Dependence of emission intensity for TPPA-BDC on temperature (298−353 K) upon λ_{ex} = 360 nm.

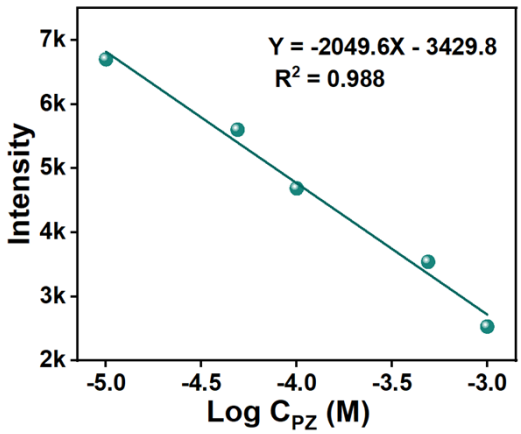

Fig. S16. Dependence of emission intensity of TPPA-BDC on concentration of PZ in aqueous solution.

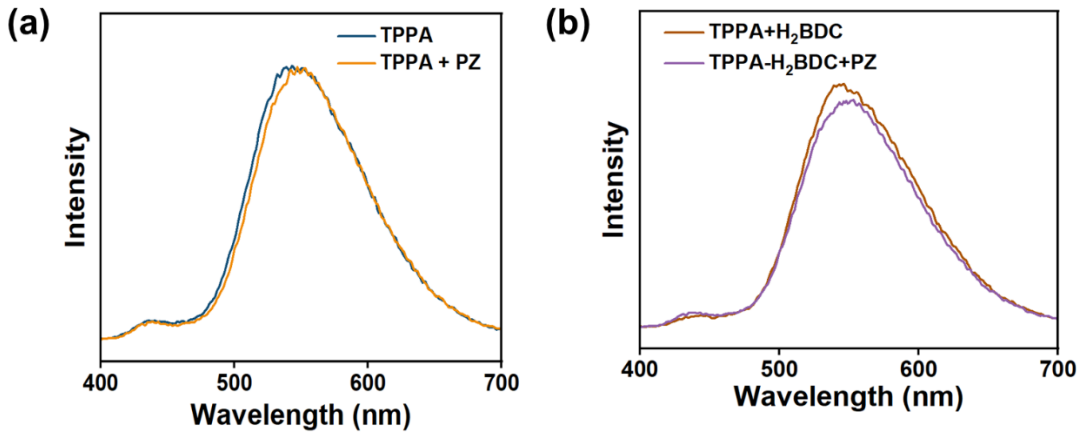

Fig. S17. (a) The emission spectra of TPPA and TPPA in PZ solution (10^{-2} M). (b) The emission spectra of TPPA+H_2BDC and TPPA+H_2BDC in PZ solution (10^{-2} M)

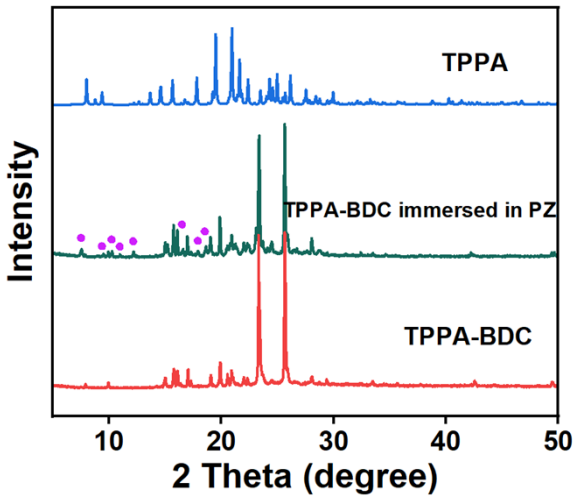

Fig. S18. PXRD patterns of TPPA-BDC, TPPA and TPPA-BDC treated with PZ (10^{-3} M). The purple dots show the new generating peaks.

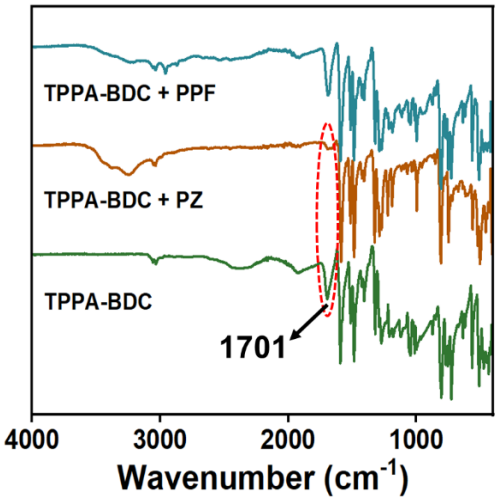

Fig. S19. FT-IR spectra of TPPA-BDC treated with PPF solution (top), TPPA-BDC impregnated with PZ solution (middle) and TPPA-BDC (bottom).

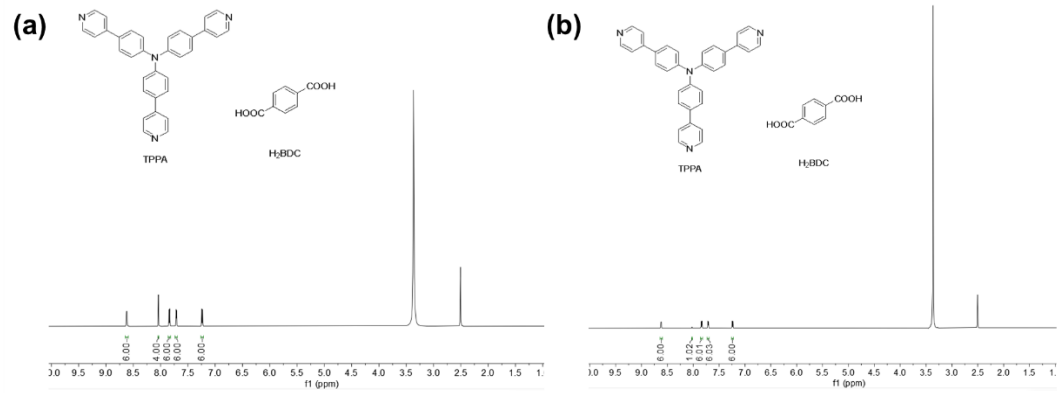

Fig. S20. ^{1}H NMR spectra of TPPA-BDC (a) and (b)TPPA-BDC treated with PZ (10^{-3} M).

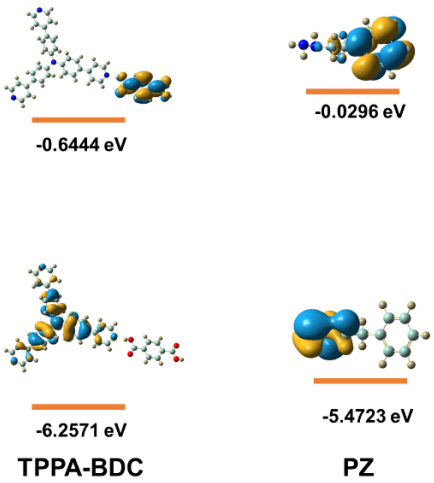

Fig. S21. The LUMO and HOMO orbitals of TPPA-BDC and PZ.

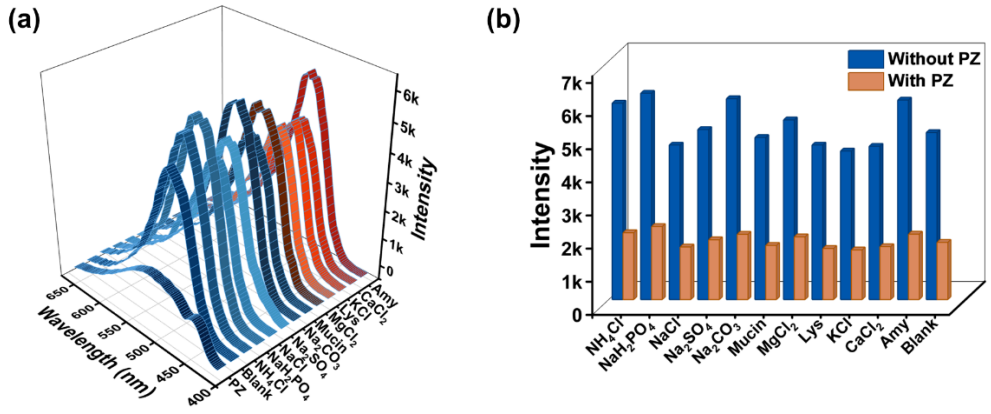

Fig. S22. (a) The emission spectra of TPPA-BDC in PZ and various components (10^{-3} M) in saliva system. (b) Selectivity and anti-interference ability of TPPA-BDC with PZ (λ_{ex} = 360 nm) in the presence and absence of different salivary components. The concentrations of PZ and salivary components are 10^{-3} M.

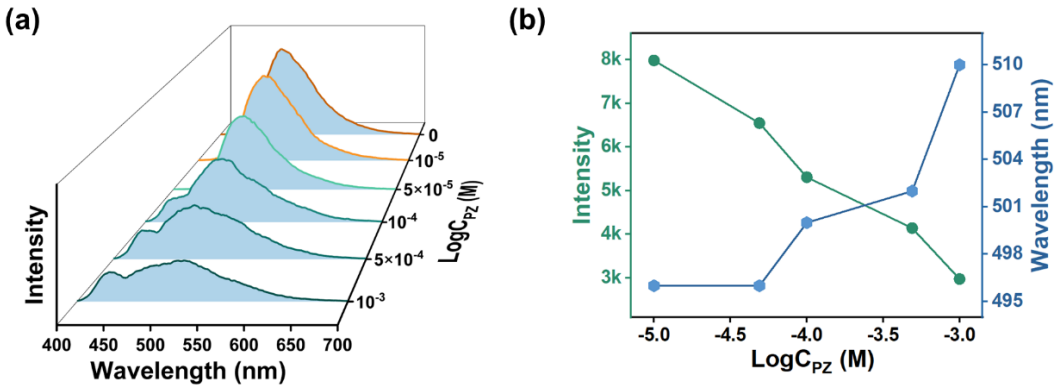

Fig. S23. (a) The fluorescence spectra of TPPA-BDC in the presence of 10^{-5}–10^{-3} M PZ in aqueous solution (λ_{ex} = 360 nm). (b) Plot of fluorescence intensity and wavelength (λ_{em}) as PZ concentration changes.

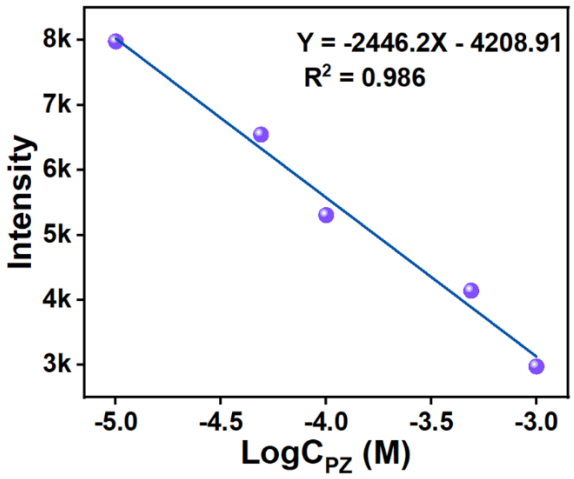

Fig. S24. Dependence of the emission intensity of TPPA-TMA on concentration of PZ in saliva.

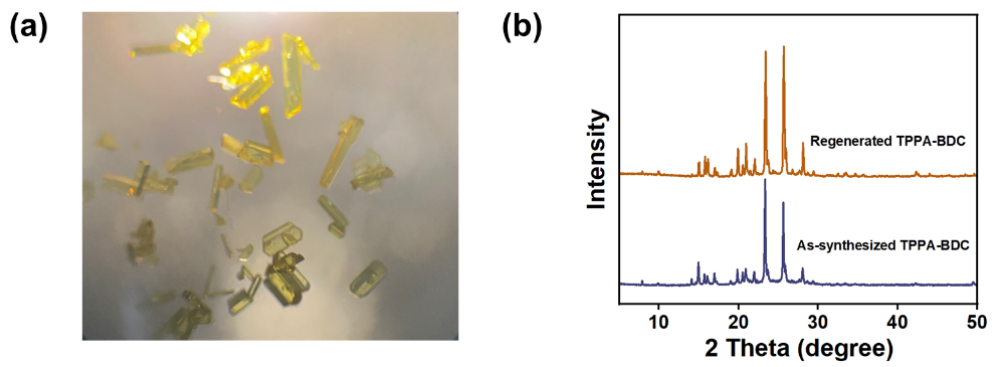

Fig. S25 (a) The picture of regenerated TPPA-BDC under the microscope. (b) PXRD patterns of as-synthesized TPPA-BDC (blue) and regenerated TPPA-BDC (yellow).

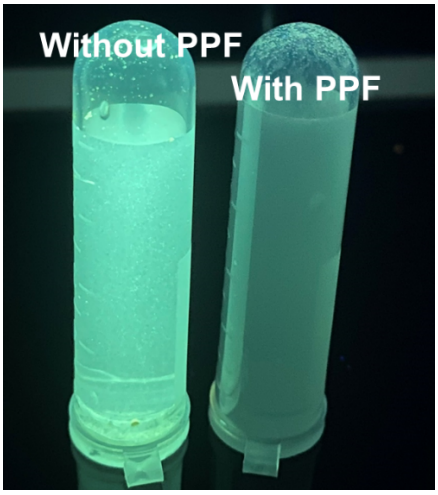

Fig. S26. The colour change of TPPA-BDC solution before and after the addition of PZ by UV lamp.

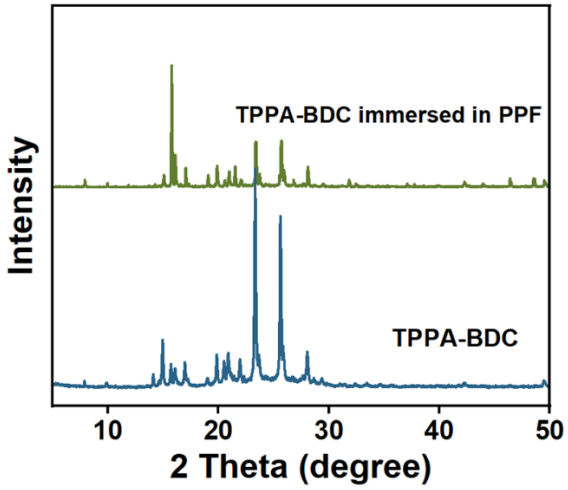

Fig. S27. PXRD patterns of TPPA-BDC (blue) and after sensing PPF (green).

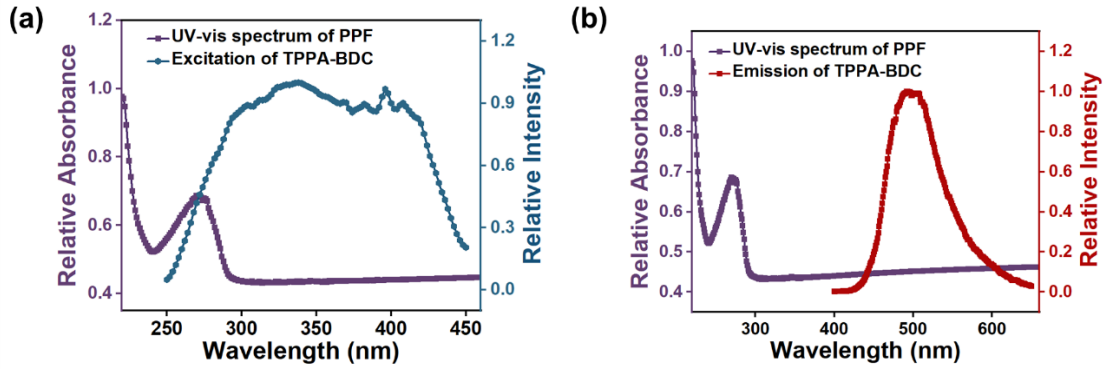

Fig. S28. The UV-Vis absorption spectra of aqueous solutions of PPF and the excitation spectrum of TPPA-BDC (a) and the emission of TPPA-BDC (b).

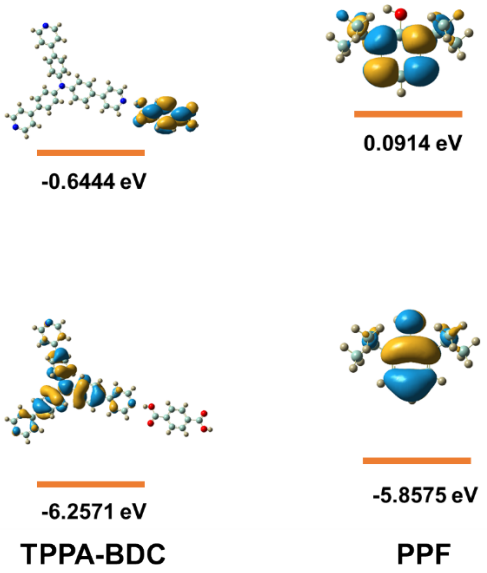

Fig. S29. The LUMO and HOMO orbitals of TPPA-BDC and PPF.

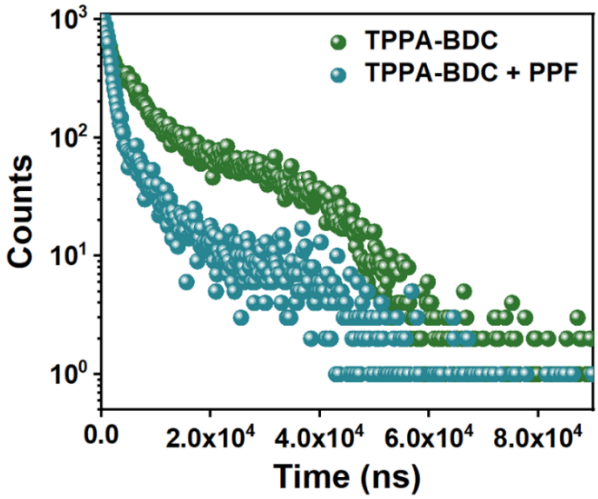

Fig. S30. Decay lifetimes of TPPA-BDC and TPPA-BDC treated with PPF.

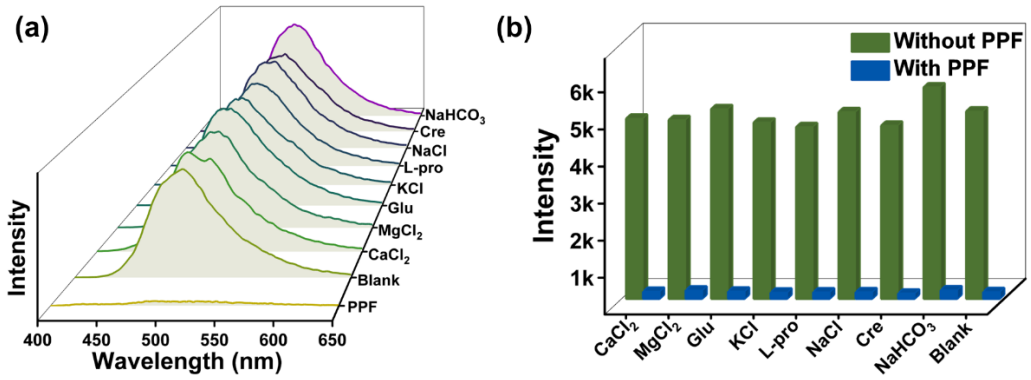

Fig. S31. (a) The emission spectra of TPPA-BDC in PPF and various components (10^{-2} M) in serum system. (b) Corresponding intensity at 496 nm for TPPA-BDC toward various components in serum system.

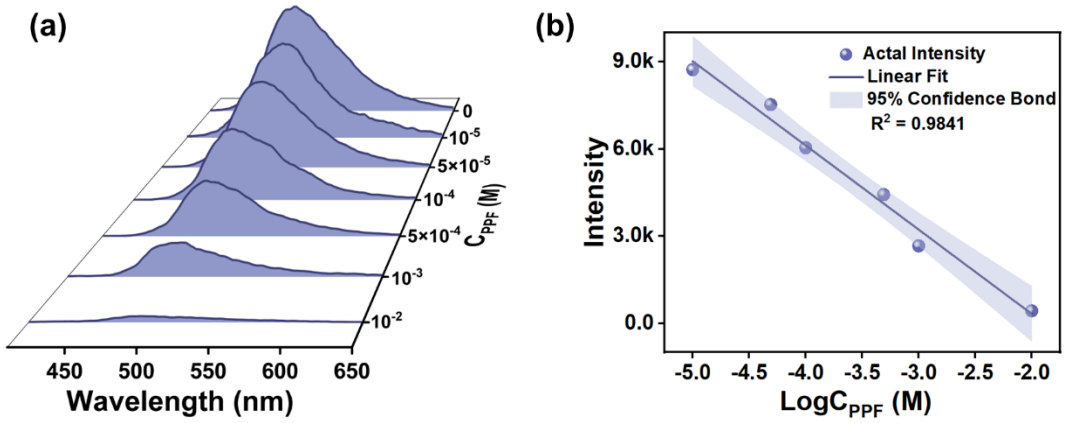

Fig. S32. (a) The emission spectrums (λ_{ex} = 360 nm) of TPPA-BDC immersed in various concentration of PPF in serum (10^{-5} – 10^{-2} M). (b) Dependence of the emission intensity of TPPA-BDC on concentration of PPF in serum.

References

[1] G. W. T. M. J. Frisch, H. B. Schlegel, G. E. Scuseria, M. A. Robb, J. R. Cheeseman, G. Scalmani, V. Barone, G. A. Petersson, H. Nakatsuji, X. Li, M. Caricato, A. Marenich, J. Bloino, B. G. Janesko, R. Gomperts, B. Mennucci, H. P. Hratchian, J. V. Ortiz, A. F. Izmaylov, J. L. Sonnenberg, D. Williams-Young, F. Ding, F. Lipparini, F. Egidi, J. Goings, B. Peng, A. Petrone, T. Henderson, D. Ranasinghe, V. G. Zakrzewski, J. Gao, N. Rega, G. Zheng, W. Liang, M. Hada, M. Ehara, K. Toyota, R. Fukuda, J. Hasegawa, M. Ishida, T. Nakajima, Y. Honda, O. Kitao, H. Nakai, T. Vreven, K. Throssell, J. A. Montgomery, Jr., J. E. Peralta, F. Ogliaro, M. Bearpark, J. J. Heyd, E. Brothers, K. N. Kudin, V. N. Staroverov, T. Keith, R. Kobayashi, J. Normand, K. Raghavachari, A. Rendell, J. C. Burant, S. S. Iyengar, J. Tomasi, M. Cossi, J. M. Millam, M. Klene, C. Adamo, R. Cammi, J. W. Ochterski, R. L. Martin, K. Morokuma, O. Farkas, J. B. Foresman, and D. J. Fox, Gaussian 09, Revision D.01; Gaussian, Inc.: Wallingford CT, 2013.

[2] S. Grimme, J. Antony, S. Ehrlich, H. Krieg, *J. Chem. Phys.* **2010**, *132*, 154104.

[3] Z. Hu, B. Yan, *J. Mater. Chem. A* **2023**, *11*, 4739-4750.